Nuclear Instruments and Methods in Physics Research A 387 (1997) 433–442

ELSEVIER

NUCLEAR INSTRUMENTS & METHODS IN PHYSICS RESEARCH Section A

Cellular automaton and elastic net for event reconstruction in the NEMO-2 experiment

NEMO Collaboration

I. Kisel[c], V. Kovalenko[c], F. Laplanche[h,*], R. Arnold[j], C. Augier[h], A. Barabash[g], D. Blum[h], V. Brudanin[c], J.E. Campagne[h], D. Dassié[a], V. Egorov[c], R. Eschbach[a], J.L. Guyonnet[j], F. Hubert[a], Ph. Hubert[a], S. Jullian[h], O. Kochetov[c], V.N. Kornoukov[g], D. Lalanne[h], F. Leccia[a], I. Link[j], C. Longuemare[b], F. Mauger[b], P. Mennrath[a], H.W. Nicholson[i], A. Nozdrin[c], F. Piquemal[a], O. Purtov[f], J.-L. Reyss[d], F. Scheibling[j], J. Suhonen[e], C.S. Sutton[i], G. Szklarz[h], V.I. Tretyak[f], V. Umatov[g], I. Vanushin[g], A. Vareille[a], Yu. Vasilyev[f], Ts. Vylov[c], V. Zerkin[f]

[a] *CENBG, IN2P3-CNRS et Université de Bordeaux, 33170 Gradignan, France*
[b] *LPC, IN2P3-CNRS et Université de Caen, 14032 Caen, France*
[c] *JINR, Dubna, Russian Federation*
[d] *CFR, CNRS, 91190 Gif sur Yvette, France*
[e] *JYVÄSKYLÄ University, 40351 Jyväskylä, Finland*
[f] *INR, Kiev, Ukraine*
[g] *ITEP, Moscow, Russian Federation*
[h] *LAL, IN2P3-CNRS et Université Paris-Sud, 91405 Orsay, France*
[i] *MHC, South Hadley, MA 01075, USA*
[j] *CRN, IN2P3-CNRS et Université Louis Pasteur, 67037 Strasbourg, France*

Received 12 May 1996; revised form received 6 November 1996

Abstract

A cellular automaton for track searching combined with an elastic net for charged particle trajectory fitting is presented. The advantages of the methods are: the simplicity of the algorithms, the fast and stable convergency to real tracks, and a good reconstruction efficiency. The combination of techniques have been used with success for event reconstruction on the data of the NEMO-2 double-beta ($\beta\beta$) decay experiments.

1. Introduction

There has been a rapid development during the last 10–15 yr of various theories of artificial neural networks. These developments are an attempt to overcome the gulf between the huge amount of factual material relating to the neurophysiology of the brain's operation and the inadequate existing mathematical formalism and computational means for a technical realization of the formalism. The brain's advantages in fulfilling recognition, logical, and computational functions come through its capability to handle tasks that are essentially parallel, nonlinear, and nonlocal operations. These capabilities have not been matched by the prevailing principle of sequential calculations with the orientation of the mathematical formalism toward locality, linearity, and stationarity of the descriptions.

The theory of artificial neural networks is essentially a part of the general theory of dynamical systems in which particular attention is devoted to the investigation of the complicated collective behavior of a very large number of comparatively simple logical objects. Included among dynamical systems are problems whose solution is complicated precisely by the nonlinearity, nonlocality,

* Corresponding author. Tel.: + 33 1 64 48 8429; fax: + 33 1 69 07 9404; e-mail: laplanche@lalcls.in2p3.fr.

PII S0168-9002(97)00097-1

discreetness, and often nonstationarity of the situation. For instance, the problems of pattern recognition and optimization appear frequently in high energy physics [1].[1] Applicable to some of the problems are cellular automata which can be regarded as a local discreet form of neural networks, and a history already exists of cellular automata in high energy physics for data filtering and track searching [2–4].

Another reason for using algorithms different from the traditional least-squares method in high energy physics is statistically grounded. Usually, the least-squares method is used to fit a particle trajectory to position measurements in such detectors as bubble chambers where errors of measurements are independent and Gaussian distributed. This is no longer valid for electronic experiments with discrete detectors which are essentially digital in character like multiwire proportional chambers and other devices. Here errors in measurements are in fact correlated and their distribution is not Gaussian [5,6]. In such cases it is better to use methods having a statistical basis corresponding to an experimental setup [7].

Even in a case of Gaussian distributed measurement errors, their statistical nature is important very often only at the final step of track tuning, whereas during the track search they are of second-order when compared with errors of tracking and can be ignored. It is thus reasonable to use simple and fast algorithms which avoid many of the problems of the least-squares method [7].

Described below is an application of a cellular automaton in searching for tracks and an elastic neural net for fitting tracks in the NEMO-2 experiment.

A typical event in this experiment has a few tracks usually well separated in space. But this situation is complicated by phenomena such as multiple scattering and hard scattering on the detector's wires. The previous tracking procedure [8] was based on the Kalman filter [9–11]. The new tracking procedure which is based on a cellular automaton and an elastic neural net was developed for the NEMO experiment during the last year. It was applied to data from the experiment so as to compare results of both tracking procedures. This comparison promoted strong confidence in the new tracking method.

In Section 2 the main features of the NEMO experiment are summarized. Section 3 presents a general description of a cellular automaton as well as a cellular automaton developed for track searching in the experiment. Section 4 introduces the elastic net method for the travelling salesman problem and its adaptation to the tracking problem. Section 5 gives the results of an application of both methods to the data from the NEMO-2 experiment. Finally, Section 6 contains a short discussion of the conclusions.

2. NEMO experiment

The goal of the NEMO collaboration [12][2] is to study double-beta ($\beta\beta$) decays of ^{100}Mo and other nuclei to probe the effective Majorana neutrino mass down to 0.1 eV. The collaboration is building the NEMO-3 detector to realize this.

The $\beta\beta$ decay process is a de-excitation of a nucleus which releases simultaneously two electrons either with or without neutrinos in the final state, $\beta\beta 2\nu$ and $\beta\beta 0\nu$, respectively. The $\beta\beta 0\nu$ decay mode, which has not yet been observed, constitutes a very sensitive test of the existence of a massive Majorana neutrino and right-handed weak currents. Thus, the observation of this process would indicate physics beyond the standard model. The $\beta\beta 2\nu$ decay, is a second order electroweak transition, and is completely described by the standard model that has already been experimentally observed. Research on this process is a useful test of the theoretical models which calculate the nuclear matrix elements. Another decay mode may also occur, $\beta\beta 0\nu\chi$, where a hypothetical light neutral boson the Majoron χ, is emitted. Decay modes which are less favorable by phase space considerations are $\beta^+\beta^+$, β^+ with electron capture, and two electron capture decays. Experimentally, the $\beta\beta$ decay modes can only be distinguished by their different electron energy spectra. The typical electron energy ranges from a few keV to a few MeV.

A prototype detector NEMO-2 [8] designed for $\beta\beta$ studies has already provided some measurements [13,15] and is presently running in the Fréjus Underground Laboratory. The detector (Fig. 1) is a 1 m^3 volume made of tracking chambers composed of drift cells operating in the Geiger mode and two plastic scintillators arrays for energy and time-of-flight measurements. The tracking volume is filled with helium gas at atmospheric pressure with 4% ethyl alcohol. Thin source foils are mounted on a 1 m^2 central frame which divides the tracking volume in two parts. On each side of the central foil are five frames composed of a pair of planes of 32 horizontal drift cells and 32 vertical drift cells. This juxtaposition of horizontal and vertical cells ensures the same tracking precision on the top and side projections of the drift chamber which are used in track reconstruction. Each octagonal Geiger cell is 32 mm in diameter and 1 m in length with a central anode wire surrounded by eight grounded wires. The efficiency of the cells is greater than 99%. The three-dimensional trajectory of a charged particle is reconstructed from longitudinal and transverse coordinates measured from the fired cells. The transverse position is given by the drift time and the longitudinal position by the plasma propagation times. The transverse resolution is 500 μm and the longitudinal resolution is 4.7 mm.

[1] http://www1.cern.ch/NeuralNets/nnwInHep.html.

[2] http://www.lal.in2p3.fr/NEMO.

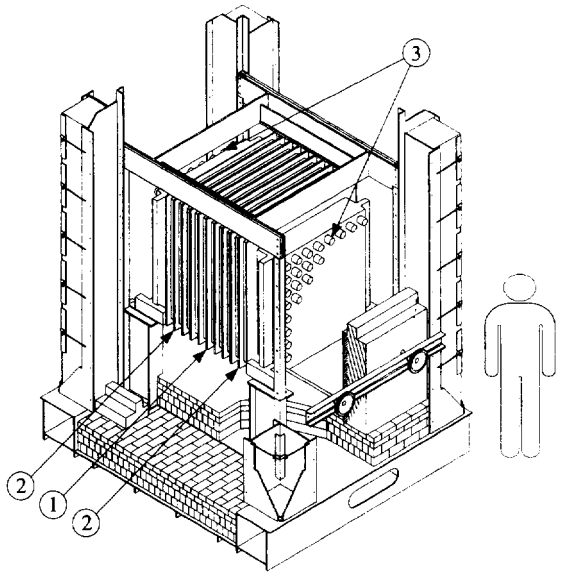

Fig. 1. The NEMO-2 prototype: 1, central frame with the metallic foil; 2, tracking device of 10 frames with 2×32 Geiger cells each; 3, scintillator walls of 5×5 counters (8×8 shown in the figure).

Peculiar to this experiment is the presence of low-energy electrons, so large multiple scattering effects have to be taken into account in the helium gas as well as hard interactions with wires of the Geiger cells. In what follows, the Geiger drift cells will be called drift tubes to avoid confusion with the cellular automaton cells.

3. Cellular automaton for track searching

Cellular automata [16] are dynamical systems that evolve in discreet, usually two-dimensional, spaces consisting of cells. Each cell can take several values. In the simplest case one has a single-bit cell: 0 or 1. The laws of evolution are local, i.e., the dynamics of the system are determined by an unchanged set of rules (for example a table) in accordance with which the new state of a cell is calculated on the basis of the states of its nearest neighbors. It is important that the change of states is made simultaneously and in parallel, with time proceeding discreetly.

Cellular automata became particularly popular in the 1970s through the publication of M. Gardner in Scientific American [17] which was devoted to Conway's game, Life.[3]

In the general case a typical cellular automaton is constructed in accordance with the following algorithm.

(i) *Define a cell and its possible discreet states*; usually, each cell has two states, 0 and 1.

(ii) *Define neighbors*; usually, each cell can communicate only with the nearest cells.

(iii) *Define rules of evolution*; these are highly dependent on the actual problem considered and usually have simple tabular forms.

(iv) *Define time evolution*; here all cells change their states simultaneously.

Using a cellular automaton for track searching, simplifies the problem and speeds up the process. As it was mentioned in the introduction one does not need to have a precise analysis of the data in the preliminary searching stages. The preliminary search for tracks involves the rough collection of experimental points which are sorted into track groups. There can be incorrect tracks constructed accidentally which will in time be rejected by additional analysis, but real tracks will not be lost.

Specific features of the experiment discussed here make the segment model of a cellular automaton perferable [4] where an elementary unit (a cell) is a segment connecting two fired wires in neighboring layers. To construct a cellular automaton for track searching in the NEMO-2 data, one follows the logic of cellular automata by defining, as below, a cell, neighbors, rules of evolution and the flow of time.

Cell: The cellular automaton is three-dimensional. A cell is identified with a straight-line segment connecting two hits in neighboring layers, thus making the cellular automaton essentially local. To take into account Geiger cell inefficiencies one must also include segments which connect hits that skip over one layer. The initial status of an event is depicted in Fig. 2(a).

Neighbors: Only segments with a common extremity can be considered as neighbors. Then owing to the detector's structure and to multiple scattering in the material and gas of the apparatus, the angles, ϕ, between track segments in the real experiment are not zero, but an upper limit ϕ_{max} can be imposed.

Rules: During evolution an integer number (position value) is associated with each cell which characterizes its position on the track. All cells are initialized with a position value of 1, and at each step of evolution each cell looks on neighbors in the previous layers and increase its position value by one unit if there is a neighbor with the same position value (Fig. 2(b)). The evolution stops when there are no more neighboring cells with the same position value. This is similar to the rule SAFE-PASS [16].

Time: Time evolves discreetly with all cells changing their states simultaneously.

At the end of the evolution the cellular automaton gives the positions of all the segments of the track candidates. The collection of the track candidates (Fig. 2(c)) is done by starting from a segment with the highest position value, adding its neighbor with a previous position value and so on.

[3] http://nuweb.jinr.dubna.su/LNP/NEMO/lifeN.html.

Upon completion of the cellular automaton, additional testing of the quality of tracks is carried out (Fig. 2(d)). This provides the rejection of "phantom" tracks which could be constructed from hits belonging to different tracks. A track is thus characterized by a number of segments and the sum of the angles between its segments. The longest smooth tracks are favoured during the test of quality.

In Fig. 3 the initial and final configurations of the cellular automaton are shown for a complicated NEMO-2 event. Two tracks which originate in the central source foil are shown. One is back-scattered on the front face of a scintillator and leaves the detector after crossing the central foil.

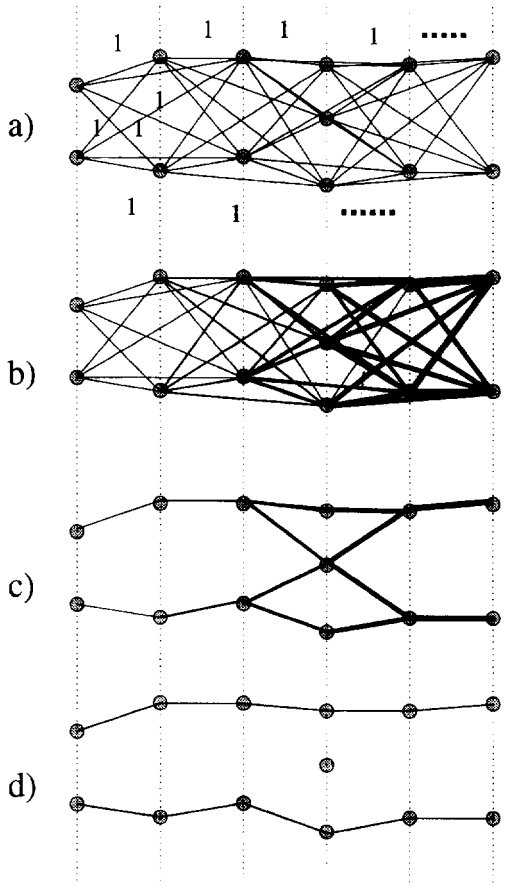

Fig. 2. Illustration of the track searching procedure with hits in six detection layers. (a) Cellular automaton initialization: all the cells or segments (see text) have a position value equal to 1. (b) End of the evolution: the position values are represented by different thicknesses of the segments. (c) Track collection: starting from cells with highest position values, tracks are collected by including segments with lower position values of one unit. Connected segments with a position value which differs by more than one are removed, and an angular cut between segments is also applied. (d) Quality test: when several branches are found the largest and smoothest track is retained.

4. Elastic net for track fitting

Described here is the elastic net method for geometrical reconstruction of charged particle trajectories with multiple scattering and hard scattering on wires. The elastic net is a kind of artificial neural network [1] which has been used for track recognition in high energy physics [18,19]. The elastic net method is well illustrated in the simple example of the travelling salesman problem. The travelling salesman problem is a classic problem in the field of combinatorial optimization, in which efficient methods for maximizing or minimizing a function of many independent variables is sought. The problem is stated as follows.

Given the positions of N cities, what is the shortest closed tour in which each city can be visited once?

All exact methods known for determining an optimal route require a computing effort that increases exponentially with the number of cities, so in practice exact solutions can be attempted only on problems involving a few hundred cities or less. The travelling salesman problem thus belongs to the large class of nondeterministic polynomial time complete problems.

One of the most successful approaches to the travelling salesman problem is the elastic net of Durbin and Willshaw [20].[4] The elastic net can be thought of as a number of beads connected by elastic to form a ring. The essence of the method is to proceed in the following fashion.

Using an iterative procedure, a circular closed path is gradually elongated non-uniformly until it eventually passes sufficiently near to all the cities to define a tour.

Denote the cities by $\boldsymbol{x}_i$ and match these cities with template coordinates $\boldsymbol{y}_a$ such that $\sum_a |\boldsymbol{y}_a - \boldsymbol{y}_{a+1}|$ is minimized and that each $\boldsymbol{x}_i$ is matched with at least one $\boldsymbol{y}_a$. Define s_{ia} to be 1 if a is matched to i and 0 otherwise. The following energy expression [21] is to be minimized in a valid tour;

$$E(s_{ia}, \boldsymbol{y}_a) = \sum_{ia} s_{ia} \cdot |\boldsymbol{x}_i - \boldsymbol{y}_a|^2 + \gamma \sum_a |\boldsymbol{y}_a - \boldsymbol{y}_{a-1}|^2 . \quad (1)$$

The γ coefficient governs the relative strength between the $\boldsymbol{x}_i$ to $\boldsymbol{y}_a$ match and the tour length. Then the dynamical equations can be written:

$$\Delta \boldsymbol{y}_a = \eta \left[2 \sum_i v_{ia} \cdot (\boldsymbol{x}_i - \boldsymbol{y}_a) + \gamma \cdot (\boldsymbol{y}_{a+1} - 2\boldsymbol{y}_a + \boldsymbol{y}_{a-1}) \right], \quad (2)$$

[4] http://nuweb.jinr.dubna.su/LNP/NEMO/tspN.html.

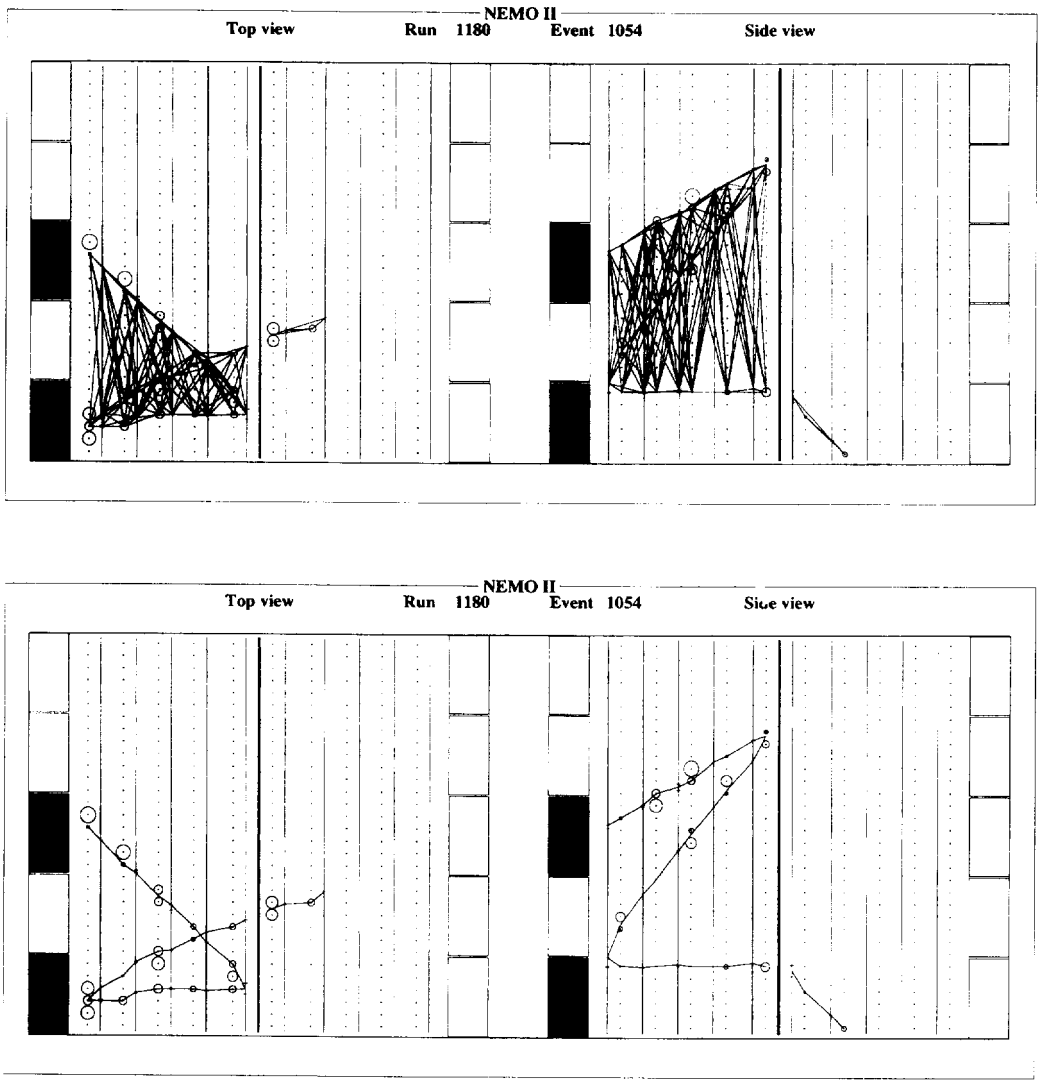

Fig. 3. Initial and final configurations of the cellular automaton for a complicated NEMO-2 event. For the drift tubes perpendicular to the figure plane, the drift distance is represented by the radius of a circle. For the drift tubes parallel to the figure plane, the small segments perpendicular to the wires indicate the trajectory position along the drift tube. Adjacent cells are assigned to clusters before starting the cellular automaton.

where Δy_a is the shifting of y_a at each step of the evolution, η is a constant, v_{ia} is a weight which characterizes the matching of a to i and is given by

$$v_{ia} = \frac{e^{-|x_i - y_a|^2/T}}{\sum_b e^{-|x_i - y_b|^2/T}}. \quad (3)$$

Here the T parameter is equated to a "temperature" which decreases during the elastic net evolution.

The algorithm is thus a procedure for the successive recalculation of the positions of a number of points of the plane in which the cities lie. The points describe a closed path which is initially a small circle centered on the middle of the distribution of cities and is gradually elongated non-uniformly to eventually pass near all the cities and thus define a tour around them, see Fig. 4 (for details see the original paper [20]). Each point on the path moves under the influence of *two types of force* (see Eq. (2):

(i) the first moves it towards those cities to which it is nearest;

(ii) the second pulls it towards its neighbors on the path, acting to minimize the total path length.

By this process, each city becomes associated with a particular section on the path. The tightness of

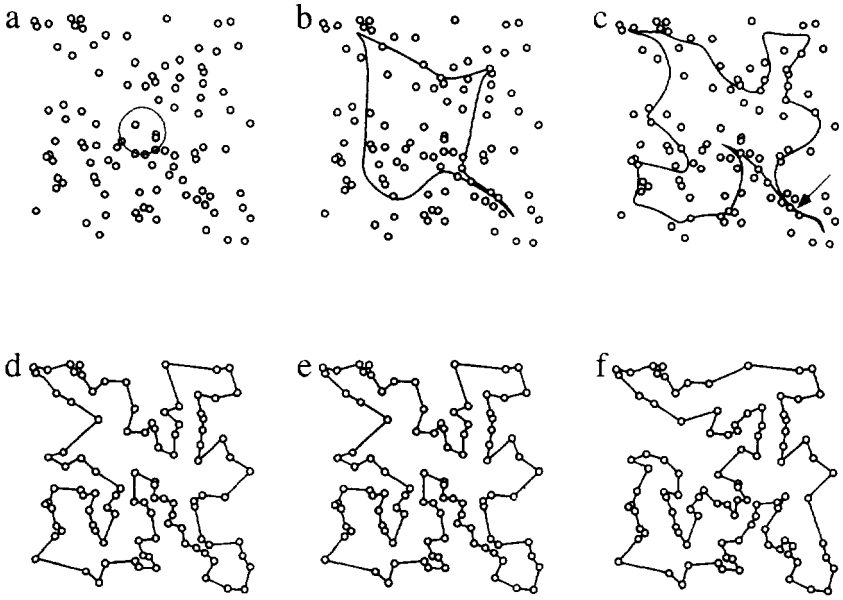

Fig. 4. Example of the progress of the elastic net method for 100 cities.

the association is determined by how the force contributed from a city depends on its distance, and the nature of this dependence changes as the algorithm progresses. Initially, all cities have roughly equal influence on each point of the path. Subsequently, a larger distance becomes less favored and each city gradually becomes more influenced by the points on the path closest to it.

To apply the elastic net method for tracking to the NEMO-2 data[5] the following process is formulated. Here it is necessary to define a track with multiple scattering as the "*most smooth*" line joining experimental points defined by hit drift tubes. Then one attempts to construct the elastic net which is a line that is deformed as in the previous example under the influence of *two types of force.*

(i) The first pulls it to the edges of the drift tube circles for which the radius is the distance of the particle path with respect to the anode wire as depicted in Fig. 5:

$$\Delta y_a^{(1)} = \alpha(y_{\text{nearest}} - y_a), \tag{4}$$

where y_a denotes the track coordinates at the ath detector plane and y_{nearest} are the coordinates of the nearest point on the edge of the drift circle with respect to y_a. At each step of the evolution the absolute value of this parameter is increasing linearly ($\alpha = 0.012 \cdot \text{iter}$) where iter is the current iteration number.

[5] http://nuweb.jinr.dubna.su/LNP/NEMO/nemoiiiN.html.

(ii) The second smoothes out the line defining the particle track:

$$\Delta y_a^{(2)} = \beta \Delta\phi, \tag{5}$$

where $\Delta\phi$ is an angle between segments at the ath plane. The β parameter is linearly decreasing during the evolution: $\beta = 0.5(1.0 - 0.05 \cdot \text{iter})$.

Even if there is no hardware noise, there will be noise due to the left–right ambiguity of drift tubes. Knowing approximately the direction of a track, one does not know whether it goes to the left or right side to a circle defined by the drift time. So at each fired wire there are two possible contact points of a track, one of which is wrong. In this case the track reconstruction task can be considered to be a problem of minimization of a function of many variables with many local minima. Most known standard methods of minimization [22] start from a point on the surface defined by a function and then minimize the function in a local area around it at each step of the iteration. In such cases there is a significant non-zero probability of stopping in a local minimum. It is possible to engage methods to escape local minima and thereby to save standard methods, but this increases the complexity of the program and makes it more unstable. The only reliable way is to start from a good initial approximation, which may not be easily found.

Contrary to standard methods, which are not always suitable, proposed here is to start from two points surrounding the global minimum and covering all the physical regions of the parameters. These points are not independent but attract each other. So the points will

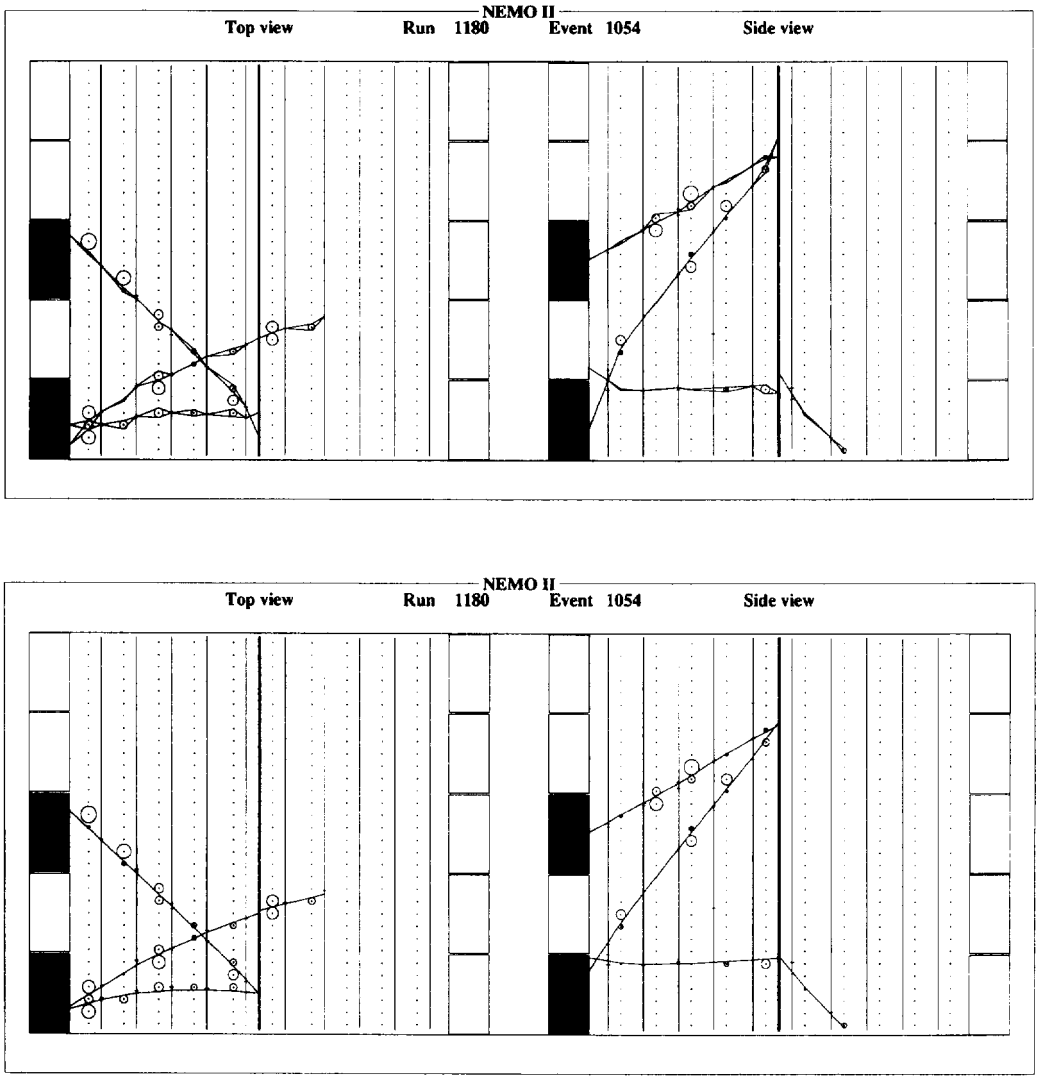

Fig. 5. Initial and final configurations of the elastic net for the NEMO-2 event already shown. Some initial configurations are eliminated by grouping hits into clusters.

pull each other from all local minima until the global minimum is reached.

In accordance with this idea one starts from two tracks which envelope the geometrical area where there is the real track. Effectively one of them touches the drift circles on the "upper side" while the other one on the "lower side". Next a *third type of force* is introduced.

(iii) An attraction between these tracks squeezes the geometrical area to get the real track:

$$\Delta y_a^{(3)} = \gamma(y_a^{\mathrm{up}} - y_a^{\mathrm{down}}), \tag{6}$$

here the γ parameter is increasing linearly during the elastic net evolution ($\gamma = 0.02 \cdot \mathrm{iter}$). This method allows one to find an optimal trajectory which corresponds to the track.

The dynamical equation of the elastic net evolution is thus

$$\begin{aligned}\Delta y_a &= \Delta y_a^{(1)} + \Delta y_a^{(2)} + \Delta y_a^{(3)} \\ &= \alpha(y_{\mathrm{nearest}} - y_a) + \beta\Delta\phi + \gamma(y_a^{\mathrm{up}} - y_a^{\mathrm{down}}).\end{aligned} \tag{7}$$

Δy_a is at each step the shifting of the point a. The convergence of the process, $|\Delta y_a| \leq 0.005\,\mathrm{cm}$ for each point a, is obtained in some tens of iterations. The evolution is stable with respect to the α, β, and γ parameters which are easily tuned.

The elastic net can be readily modified to reconstruct hard scattering tracks. Here one has only to switch off track smoothing at hard scattering points which are found during the preliminary analysis. Fig. 5 presents

initial and final configurations of the elastic net for the same NEMO-2 event shown in Fig. 3.

5. Results

In the NEMO-2 experiment the source plane is divided into two halves. The first is a 152 g isotopically enriched cadmium foil (93.2% is ^{116}Cd, which is a $\beta\beta$ emitter) with a thickness of 40 μm. The second-half is a 143 g foil of natural cadmium of which 7.49% is ^{116}Cd and used for the background measurement. The complete data set (6588 h of running time) was previously processed using a tracking procedure based on the Kalman filter [9]. The data have been accepted for publication [15] and an earlier result drawn with 40% of the data set has already been published [14]. The new tracking method presented here was used to process the data a second time.

An electron is defined by a track linking the source foil and one scintillator. The maximum scattering angle along the track has to be less than 20 to reject hard scattering situations. A photon is recognized as one or two adjacent fired scintillators without an associated particle track. For photons and electrons an energy deposited greater than 200 keV in the calorimeter is required in order to obtain sufficiently good timing resolution. In the analysis of two-electron events a cut on the angle between the two electron tracks is applied ($\cos\alpha < 0.6$). Also, in the analysis a two-electron event is identified as (2e) and electron–photon event as ($e\gamma$).

In the coordinate system of the detector the origin of the axes is at the center of the source plane with the x-axis being horizontal and the y-axis vertical. The positioning of the enriched cadmium foil is such that it has an event vertex x coordinate in the range 1.0–47.5 cm. Both foils are symmetrical with respect to the y-axis. The event y vertex has to be within the limits 0 ± 47.5 cm. In the case of 2e events, the difference between the vertex position of each track was required to be less than 5 cm. This condition was imposed due to multiple scattering which leads to a vertex position difference of 1 cm (rms) for a 200 keV electron.

After applying the cuts to extract the $\beta\beta2\nu$ candidates with the new tracking method, 232 two-electron events were selected in the enriched foil, 61 in the natural one including 14.8 calculated $\beta\beta2\nu$ events. With the Kalman filter tracking method, these numbers were 219, 58 and 13.6, respectively. The Monte-Carlo simulation data of the $\beta\beta2\nu$ decay in the NEMO-2 detector was also analysed using the two tracking programs. With the new method an efficiency of 1.88% for extracting the two-electron events is obtained instead of 1.73% with the current tracking algorithm. The number of events entering the half-life calculation is 185.8 with the new tracking method and 174.6 with the Kalman filter. The same half-life was computed in both cases. This comparison promotes strong confidence in the new tracking method. The track fitting can provide in both methods slightly different track parameters. The most sensitive parameters used in the data analysis are: the vertex position on the source foil, the intersection coordinates of the extrapolated trajectory with the scintillator arrays and the large angle scattering in the tracking chambers. The difference between the numbers of selected events in both methods is mainly due to the cuts applied to the above parameters which are sometimes better determined with the new tracking method.

In summary, the main features of the tracking program based on the cellular automaton and elastic net methods are:

- An increase by a factor 5 in the processing speed (70 events/s for off-line analysis while on-line processing, without reading from and writing to disk, yields 350 events/s).
- Working in 3D space to separate close tracks in a projection (this is also true for Kalman filter).
- Good reconstruction of tracks with hard scattering on wires.
- Reconstruction of short tracks (with as few as 2 planes involved).
- Simple to modify by introducing additional criteria in the analysis.

Using the NEMO-2 data but without applying any cuts, selected figures (Figs. 6–11) are presented below to illustrate some characteristics of the tracking method and of the data taken with the detector.

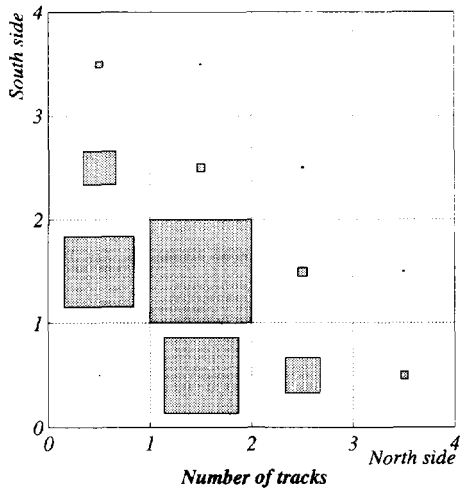

Fig. 6. Track multiplicity. (North and South refers to the sides defined by the source plane.) The large number of events with one track on each side is due to single electrons crossing the source. Most of the one track events come from Compton electrons produced in the source. Higher multiplicities are mainly due to the Möller effect in the source.

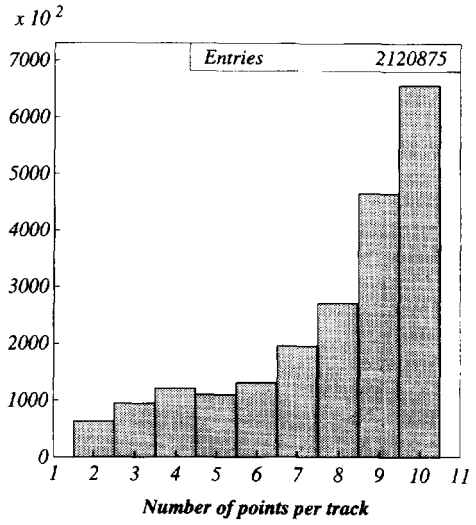

Fig. 7. Distribution of the number of points per track. There are ten detection planes between the source and a scintillator array but very short tracks, when a charged particle crosses only two planes, are also reconstructed.

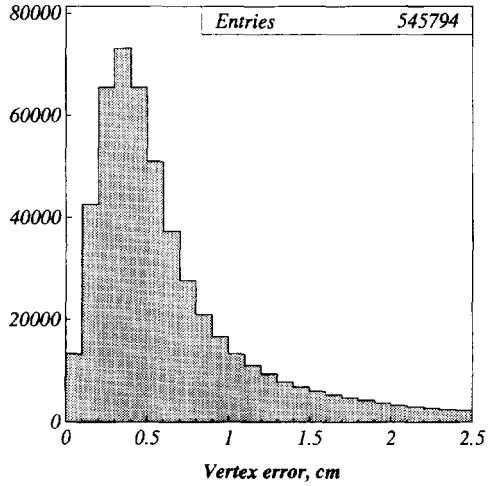

Fig. 9. Vertex uncertainty distribution extracted from two-track events. The precision of the vertex position is not crucial in the experiment. The tail of the distribution is due to very short tracks and/or hard scattering on wires close to the source (first detection plane).

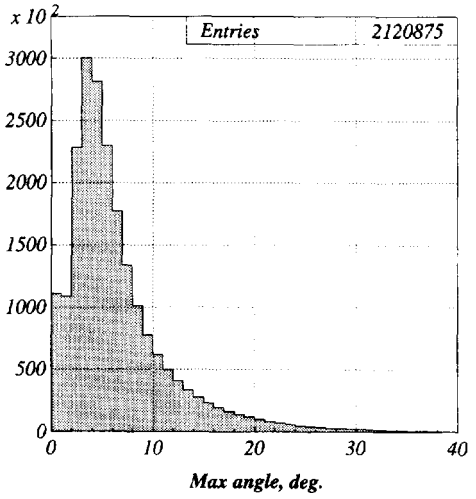

Fig. 8. Maximum angle distribution between track segments. A multiple scattering angle of a few degrees is measured for low energy electrons involved in natural radioactivity processes. The tail of the distribution is due to hard scattering on the Geiger cell wires.

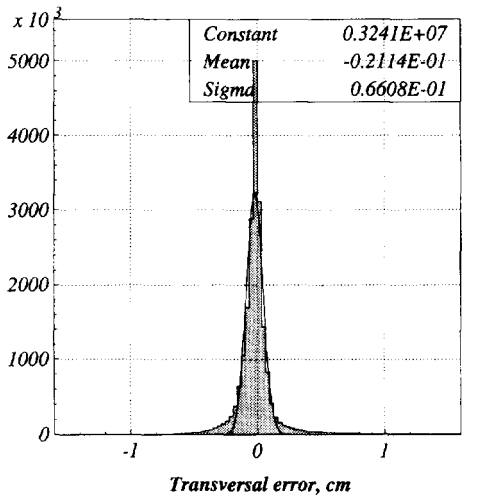

Fig. 10. Residuals in transverse direction. In a plane perpendicular to the wires, the distance between the track and the measured position of the hits is plotted. The peak at zero cm is mainly due to short tracks.

6. Conclusions

The results of the application to real NEMO-2 events demonstrate reliable operation of the cellular automaton and elastic net methods in the case of multiple scattering in a gas and hard interactions on wires in the tracking detector.

The advantages of the methods are:

- simplicity of the algorithms;
- high reconstruction efficiency;
- fast and stable convergency to real tracks.

In the next stage of this investigation a detector with a magnetic field will be taken into account to develop algorithms for the NEMO-3 [12] experiment. The plan is to use the cellular automaton technique in the on-line operation of the detector.

Detailed description of the NEMO experiment and software are available in the NEMO Home page

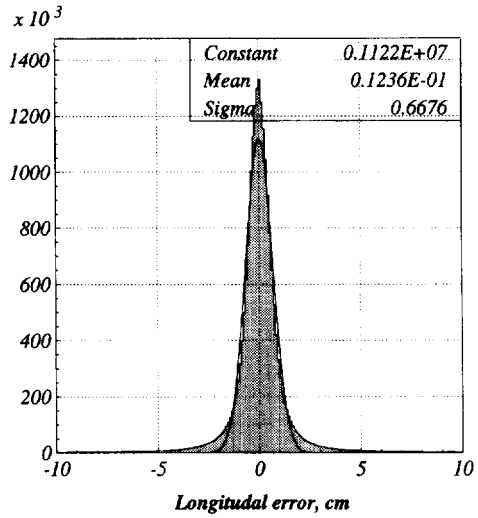

Fig. 11. Residuals in longitudinal direction. The precision in this projection comes from the time fluctuations of the Geiger plasma along the anode wire which is 1 m long.

in Dubna.[6] Using Netscape one can find there Java applets animating the game Life, the elastic net for the travelling salesman problem, the elastic net for tracking and a selection of other topics.

Acknowledgements

A. Budnik and T. Filipova are acknowledged for this work.

References

[1] I. Kisel, V. Neskoromnyi and G. Ososkov, Phys. Part. Nucl. 24 (1993) 657.
[2] I. Kisel and G. Ososkov, Proc. Int. Conf. on Computing in High Energy Physics CHEP92, Annecy, France, 1992, CERN-92-07 (1992) 646.
[3] A. Glazov, I. Kisel, E. Konotopskaya and G. Ososkov, Nucl. Instr. and Meth. A 329 (1993) 262.
[4] M.P. Bussa, L. Fava, L. Ferrero, A. Grasso, V. Ivanov, I. Kisel, E. Konotopskaya and G. Pontecorvo, Nuovo Cimento A 109 (1996) 327.
[5] I. Duerdoth, Nucl. Instr. and Meth. 203 (1982) 291.
[6] F. James, Nucl. Instr. and Meth. 211 (1983) 145.
[7] N. Chernov, A. Glazov, I. Kisel, E. Konotopskaya, S. Korenchenko and G. Ososkov, Comp. Phys. Commun. 74 (1993) 217.
[8] R. Arnold et al. (NEMO Collaboration), Nucl. Instr. and Meth. A 354 (1995) 338.
[9] P. Billoir, Nucl. Instr. and Meth. 225 (1984) 352.
[10] P. Billoir, R. Frühwirth and M. Regler, Nucl. Instr. and Meth. A 241 (1985) 115.
[11] R. Frühwirth, Nucl. Instr. and Meth. A 262 (1987) 444.
[12] NEMO Collaboration, NEMO-3 Proposal, Preprint LAL 94-29, 1994.
[13] D. Dassié et al. (NEMO Collaboration), Phys. Rev. D 51 (1995) 2090.
[14] R. Arnold et al. (NEMO Collaboration), JETP Lett. 61 (1995) 170.
[15] R. Arnold et al. (NEMO Collaboration), Z. Phys. C 72 (1996) 239.
[16] T. Toffoli and N. Margolus, Cellular Automata Machines: A New Environment for Modelling (MIT Press, Cambridge, MA, 1987).
[17] M. Gardner, Sci. Amer. 223 (1970) 120.
[18] M. Gyulassy and M. Harlander, Comp. Phys. Commun. 66 (1991) 31.
[19] M. Ohlsson, C. Peterson and A.L. Yuille, Comput. Phys. Commun. 71 (1992) 77.
[20] R. Durbin and D. Willshaw, Nature 326 (1987) 689.
[21] C. Peterson and T. Rögnvaldsson, Introduction to artificial neural networks, CERN School of Computing, Ystad, Sweden, 23 August–2 September 1991, CERN 92-02 (1992) p. 113.
[22] W.H. Press, B.P. Flannery, S.A. Teukolsky and W.T. Vetterling, Numerical Recipes: the Art of Scientific Computing (Cambridge University Press, 1986).

[6] http://nuweb.jinr.dubna.su/LNP/NEMO.